Precision Radial Velocity Spectrograph for the infrared

Hugh R.A. Jones[a], John Rayner[b] , Larry Ramsey[c], David Henry[d], Bill Dent[d], David Montgomery[d], Andy Vick[d], Derek Ives[d], Ian Egan[d], David Lunney[d], Phil Rees[d], Adrian Webster[e], Chris Tinney[f], Mike Liu[b]

[a] Centre for Astrophysics Research, University of Hertfordshire, Hatfield, UK;
[b] Institute for Astronomy, University of Hawaii, USA;
[c] Penn State University, State College, PA 16802, USA;
[d] Astronomy Technology Centre, Royal Observatory, Edinburgh, UK;
[e] Institute of Astronomy University of Edinburgh, Edinburgh, UK;
[e] University of New South Wales, Sydney, Australia.

ABSTRACT

We present a conceptual design for a Precision Radial Velocity Spectrograph (PRVS) operating in the infrared. PRVS is a fibre fed high resolving power (R~70,000 at 2.5 pixel sampling) cryogenic echelle spectrograph operating in the near infrared (0.95 – 1.8 microns) and is designed to provide 1 m/s radial velocity measurements on Gemini but is envisaged with the ability to feed other Mauna Kea telescopes. We identify the various error sources to overcome in order to the required stability. We have constructed models simulating likely candidates and demonstrated the ability to recover exoplanetary RV signals in the infrared. PRVS should achieve a total RV error of around 1 m/s on a typical M6V star. We use these results as an input to a simulated 5-year survey of nearby M stars. Based on a scaling of optical results, such a survey has the sensitivity to detect several terrestrial mass planets in the habitable zone around nearby stars. PRVS will thus test theoretical planet formation models, which predict an abundance of terrestrial-mass planets around low-mass stars. We have conducted limited experiments with a brass-board instrument on the Sun in the infrared to explore real-world issues achieving better than 10 m/s precision in single 10 s exposures and better than 5 m/s when integrated across a minute of observing.

1. FINDING TERRESTRIAL-MASS PLANETS AROUND LOW-MASS STARS

The radial velocity technique has played the dominant role in foundation of this new field. Surveys using this method have discovered almost all the planets known within 200 pc, and the vast majority of gas-giant planets found within 3 AU of their host stars. Other techniques, such as searches for planetary transits and gravitational micro-lensing events have so far had limited success, although many of these programs have begun only recently. Doppler searches, however, provide the most accurate estimates of key exoplanet properties: minimum planet mass, orbital period, orbital semi-major axis and eccentricity. They also differ from photometric transit and micro-lensing surveys because they specifically target nearby well characterised stars. They provide robust minimum masses and orbital parameters and allow for critical and independent verification by other groups and techniques. One of the key results coming out of the Doppler surveys so far is that low-mass planets are much more common than high-mass ones[1] and that exoplanets form with masses at least as low as Neptune. Improvements in the efficiency and sampling of searches at optical wavelengths promise long-term precisions of ~0.5 m/s and ~5 $M_\oplus$ detections around solar-type stars. While this may be the limit for CCD-based surveys of solar type stars until larger telescopes become available it is nonetheless feasible to survey lower mass primaries to achieve a corresponding smaller mass limit. Thus the lowest mass Doppler signals have been found around M dwarfs (e.g., GJ876d[2] 7 $M_\oplus$) and detections down to a few $M_\oplus$ detections should be feasible around mid-type M dwarfs. This is the PRVS approach, to search around lower-mass primary stars since the RV reflex signal will be larger for lighter primary stars.

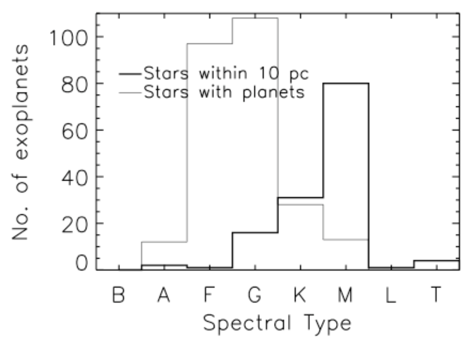

Figure 1. Number of exoplanets known per spectral type based on exoplanets.org shown with thin line. The thick line shows the breakdown of stars within 10pc (still incomplete for M dwarfs) from http://www.chara.gsu.edu/RECONS/TOP100.htm. While M dwarfs dominate the Solar neighbourhood, few exoplanets have yet been discovered in orbit around them.

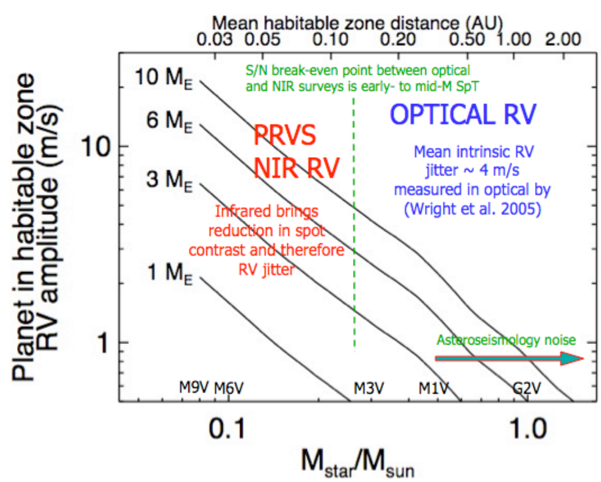

Figure 2. Radial velocity amplitude as function of host mass or mean habitable zone distance comparing PRVS with optical radial velocity surveys.

Circumstellar disks appear to be common around young (few Myr) low-mass stars and brown dwarfs (e.g. Liu, Najita & Tokunaga 2003[4]), naturally raising the question of whether these objects can form planets and, if so, how their planetary systems compare to the well-studied systems around solar-type stars. Since 8 out of 9 stars in a volume-limited sample are M dwarfs (e.g. Figure 1), it is imperative to assess the planet-bearing frequency of what may be the most common sites of extra-solar planetary systems. In fact GJ876d and the microlensing detection of the distant 5 Earth-mass exoplanet OGLE-2005-BLG-390Lb (Beaulieu et al. 2006[3]) indicate that exoplanets near terrestrial-mass do exist. Thus a major new frontier in exoplanet research is to find and characterise the local examples. Apart from their proximity, M dwarfs are particularly interesting because they offer the possibility to detect terrestrial mass planets in their habitable zone. **Figure** 2 indicates that optical RV surveys are restricted to stars more massive than about M4 dwarfs (~0.3 $M_{\odot}$). Very nearby, lower mass M dwarfs are optically too faint (e.g. the lowest mass planet detected to date by RV has a 1.9 d period and is around Gl876d, an M4 star at 4.7pc; this required regular monitoring on Keck from 1997 to 2005 and data on 6 consecutive nights[2]). In order to optimise the choice of wavelength and spectrograph resolution we examined the radial velocity information in late-type M dwarfs (Figure 3).

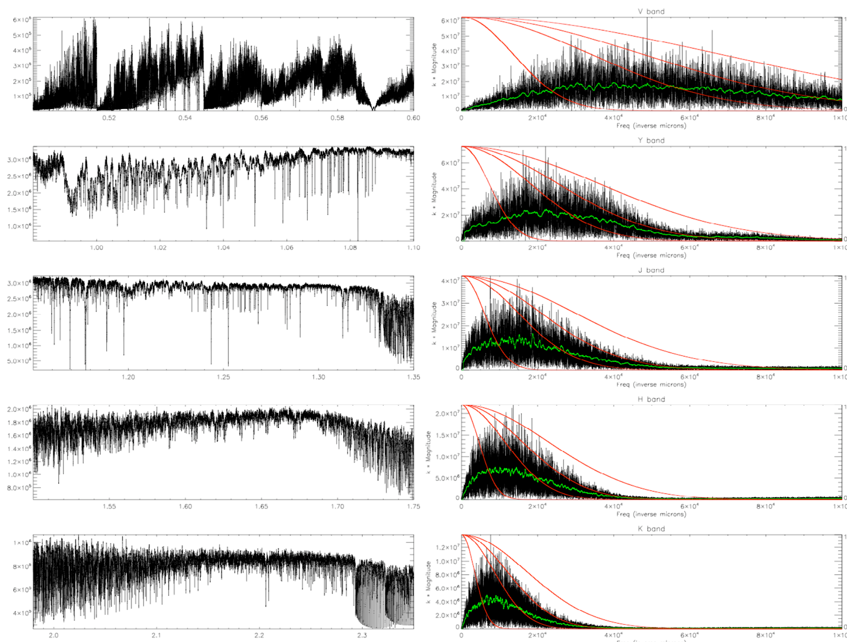

Figure 3. Doppler information in 5 spectral regions of an M6V star V+R, Y, J, H and K. On the left are the theoretical spectra for the regions and on the right are the Fourier transforms of the derivatives dF/dλ as a function of spatial frequencies. The overplotted curves are the transforms of Gaussian spectral response functions with R=20, 50, 70, and 100k (left to right). These curves indicate that a resolving power of ≥ 70k is needed to capture the Doppler information contained in the broad peak. However, increasing the resolving power to 100k provides little additional gain, as this resolving power serves only to capture more information in the weak tail of the distribution.

2. PRVS DESIGN

Light from the telescope is re-imaged onto the entrance of an optical fibre located in the Fibre Deployment and Acquisition System (FDAS) which is mounted on the ISS near to the calibration unit (GCAL) at the f/16 cassegrain focus. A CCD fibre-viewing camera is used for acquisition and guiding. The 60 m long ‘object’ fibre runs from the FDAS through the telescope cable wrap down to the telescope pier laboratory and into a bench-mounted spectrograph. For environmental stability the spectrograph is contained inside a vacuum jacket and is temperature controlled. The bulk of the spectrograph is cooled to 190 K. A second ‘reference’ fibre runs from a calibration unit located next to the cryostat into the spectrograph. A third ‘calibration’ fibre feeds calibration light up to the FDAS so that calibration light can also be transmitted through the object fibre when selected. The object and reference fibres are terminated at the cryostat and are optically coupled into the cryostat to form a pseudo-slit at the entrance of the spectrograph. Starlight from the object fibre is dispersed in the spectrograph and forms the object spectrum side-by-side with a wavelength reference spectrum formed by dispersed arc line light from the reference fibre. Radial velocity is measured by measuring the wavelength shift of the object spectrum relative to the simultaneously exposed wavelength reference spectrum. Figure 4 shows a schematic layout of PRVS.

Two detector systems are used. The spectrograph detector is a 1x2 mosaic of 2048x2048 ~0.9-1.75 µm devices. For object acquisition and slow guiding a 512x512 CCD camera is used.

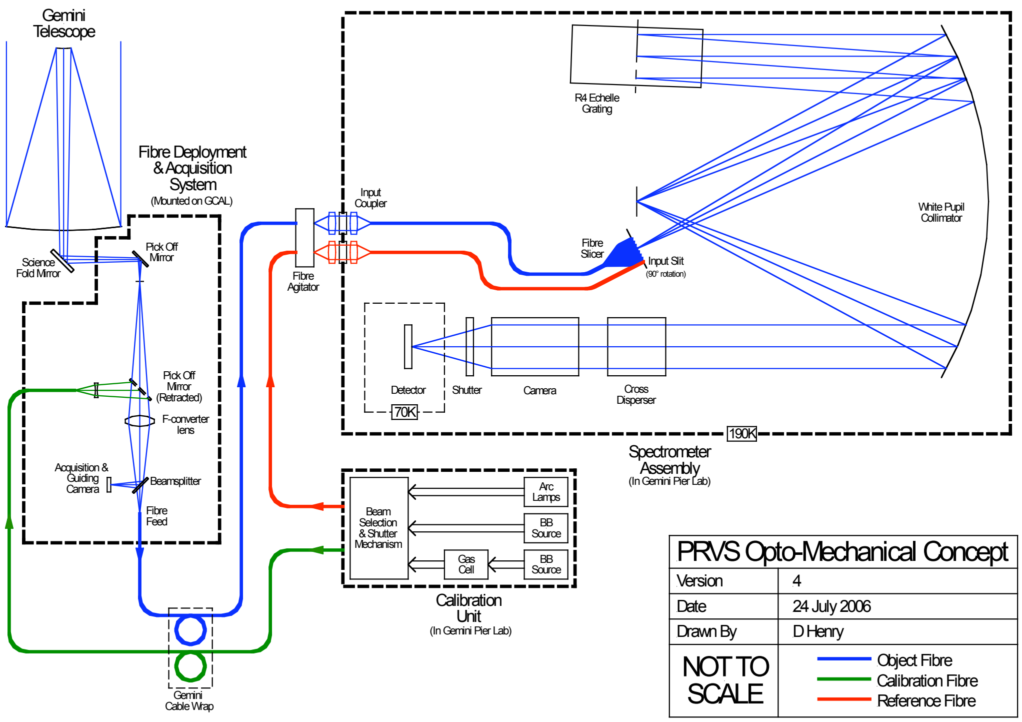

Figure 4. PRVS Opto-mechanical Block Diagram

2.1 Fibre deployment and acquisition system

The Fibre Deployment and Acquisition System is mounted on the ISS close to GCAL. This system re-images the telescope focal plane onto the object fibre and uses a CCD camera (the Fibre Viewer) for object acquisition and slow guiding. It also projects calibration light into the object fibre when required.

The science fold mirror sends the beam to GCAL where a small pickoff mirror sends the f/16 beam to a focal reducing achromatic doublet lens (see Figure 4). This lens re-images the telescope focal plane at f/5.5 onto the object fiber. A focal ratio of f/5.5 is chosen to minimize focal ratio degradation. The fibre is 300 µm in diameter and only uses 1.4″ of the re-imaged field. For median seeing of about 0.6″ at J the light loss (spill-over from the object fibre) is about 2%.

A CaF2 substrate located behind the lens reflects about 1.5% of this beam through a Z-band (0.83-1.00µm) filter and onto a CCD (the Fibre Viewer). The bare substrate reflects enough signal for acquisition and guiding on our faintest RV targets (L2 dwarf 50σ1sec=14.8 at Z, 50% QE) while at the same time minimizing the light loss in the spectrograph path. The brightest stars in the RV survey are early M dwarfs (Z magnitude <5.0) and require additional filtering (Z plus neutral density filter) to avoid saturation in the shortest on-chip integration times of about 0.1 s. This requires a simple filter wheel or slide in front of the CCD camera.

There is a small position offset between the guiding (Z) and observing wavelengths (YJH) due to atmospheric dispersion (about 0.15″ between Z and J at an airmass of 1.5). This is corrected for in software. At an image scale 0.06″/pixel (13µm) a 512x512 CCD format gives a FOV 31″x31″. The lens, substrate, fibre, and CCD are all rigidly mounted and so there is no significant relative flexure (< one CCD pixel/hour). Any flexure in the pickoff mirror acts like a simple guiding error.

When the pickoff mirror is in its retracted position the output of the calibration fibre is re-imaged onto the input of the object fiber at f/5.5. Calibration light (arcs, continuum, continuum plus gas cell absorption) in the object fibre is observed before and after observing the science object.

2.2 Fore-optics fibre Assembly

Starlight from the telescope focal plane is re-imaged onto the end of the object fibre at a focal ratio of f/5.5 to minimize focal ratio degradation. The 300 µm diameter object fibre runs from the FDAS through the cable wrap to the cryostat located in the telescope pier laboratory, requiring a fibre length of about 60 m. The 100 µm diameter reference fibre runs from the Calibration Assembly to the cryostat, requiring a length of a few meters. The calibration fibre runs from the Calibration Assembly to the Fibre Deployment and Acquisition Assembly, along the same path as the object fibre (see Figure 5).

Immediately outside the entrance to the cryostat the object and reference fibres pass through a mechanical agitator to remove modal noise and to increase spatial scrambling. This device agitates the fibres at a frequency of about 60 Hz and at an amplitude of a few hundred microns. There is about 1 m length of fibre from the image slicer input to the pseudo slit. To remove modal noise this cable is run through magnetic beads that are slightly vibrated through the cryostat vacuum jacket via an electromagnet outside the jacket.

2.3 Spectrograph

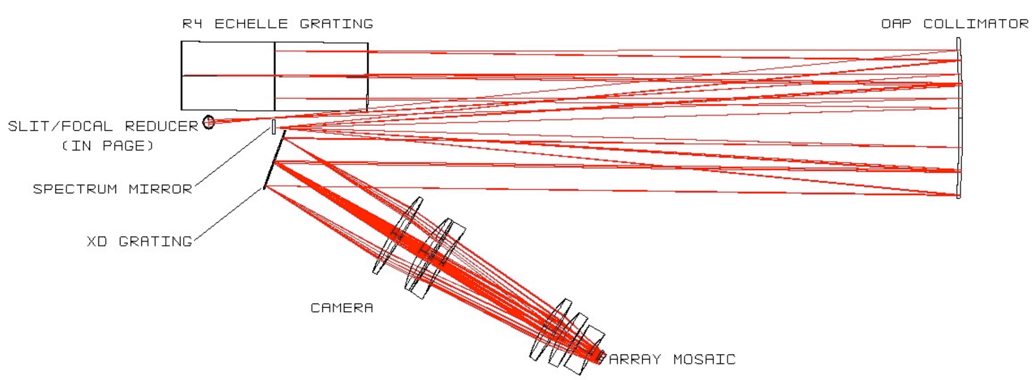

Figure 5. Spectrograph layout

The optical design of the spectrograph is similar to other white pupil spectrographs such as UVES on the VLT, MRS on the HET and, in particular, HARPS on the ESO 3.6m La Silla telescope. The layout of the spectrograph is shown in Figure 5. The f/5.5 beam exiting from the pseudo-slit is reduced to about f/14 by the focal reducer doublet lens. The slower beam is needed to control aberrations in the spectrograph. A large off-axis parabolic (OAP) mirror then collimates the beam and forms a 140 mm diameter white pupil on the echelle grating. The OAP collimator has a focal length of 2000 mm and a rectangular clear aperture of 500 mm x 446 mm. For thermal stability all the mirrors and gratings are made from Zerodur.

For a resolving power of R=70,000 an R4 31.6 lines/mm echelle grating is required (162 mm x 552 mm). This is the same as used in HARPS, UVES and some other spectrographs. Grating illumination is in pseudo-Littrow mode with an off-plane angle of γ =0.4°. This is optimum for throughput but does introduce a small tilt of about 3° of the re-imaged slit on the detector.

Following dispersion at the grating a second reflection in the OAP forms a dispersed image of the slit on the spectrum mirror (clear aperture 386 mm x 30 mm) that is located next to the echelle. The beam from the spectrum mirror is reflected for a third time in the OAP and forms a second white pupil on the cross-dispersing grating located close to the spectrum mirror. The cross-disperser is a first-order plane grating (100 lines/mm, blaze angle 4°). It is tilted 20° to allow the reflected beam to clear the input beam.

The dispersed beam from the cross disperser is imaged onto the array mosaic by a six-element f/3 refractive camera. All the lenses have spherical surfaces and are made from standard optical glasses with diameters ranging from about 100 mm to 260 mm. An order-sorting filter is the last optical element before the detector. Image quality at the detector is very good with RMS spot diameters < 9 μm (including tolerancing) compared to the re-imaged slit width at the detector of 45 μm (2.5 pixels). Therefore the spectrograph image quality only degrades the resolving power by 2%.

In the baseline design a 1x2 mosaic of H2RG 2048x2048 detectors (18μm pixels) covers most of the YJH spectral range simultaneously at R=70,000 with 2.5 pixel sampling, and with sufficient separation between orders to accommodate the image-sliced slit containing the object and reference fibre.

2.4 Cryostat

The design consists of a vacuum vessel (~3.3 m x 1.7 m x 1.25 m, volume 2.8 m^3) supported on anti-vibration supports of the type used on optical benches. An optical support structure is mounted within the vacuum vessel on an isolating flexure system. The flexure system supports a radiation shield that encloses the optical support structure. It also thermally insulates the optical support structure from the radiation shield. The optical components are mounted within substructure modules, and these in turn are mounted to the optical support structure in a semi-kinematic way. The optical bench and radiation shield are maintained at the operating temperature of 190 K and stabilised to better than 0.05 K by combining a vibration-isolated CTI-1050 closed-cycle cooler with servo controlled resistive heating elements on the optical bench. Liquid Nitrogen plumbing and a dewar is provided to pre-cool the radiation shield and the optical bench. The second stage of the closed-cycle cooler maintains the array mosaic at ~70 K and stabilised to better than 0.01 K. A window/feed-through provides the interface for the fibre coupling. There are also breakout panels for the instrument vacuum services, electrical services and detector signal cabling.

The total mass of the cryostat is 1705 kg, comprising of the cold structure 863 kg (optical bench and components 411 kg, radiation shield 452 kg), vacuum vessel 747 kg, legs 45 kg, and fasteners 50 kg.

2.5 Anticipated PRVS error budget

Table 1. Errors arising from analysis of the proposed PRVS design.

Error source	**Contribution**	**Comment**
Drift measurement with sim. arcs	< 0.2 m/s	~ 300 arc lines typically > 60 s
Photon-weighted centre of integration	< 0.1 m/s	Median sky conditions (1m/s corresponds to 30s)
Wavelength calibration	< 0.1 m/s	> 1000 arc lines during daytime calibration
Instrument SRF measurement	< 0.3 m/s	> 1000 arc lines during daytime calibration
Opto-mechanical stability	< 0.3 m/s	< 0.1 pixel drift during an observation
Centring and guiding	< 0.3 m/s	Spatial scrambling of fibre and CCD guiding
Background subtraction	< 0.1 m/s	Stability of background, dark current, bias etc.
Total instrument noise	**< 0.6 m/s**	RMS
Source photon noise	0.8 m/s	m_Y=10.5 M6 V ($v\sin i$=5 km/s) S/N=300 in 14 min
Source radial velocity jitter	(0-20 m/s)	Sources selected for minimum intrinsic noise
Atmospheric noise	~ 0.5 m/s	Modelled effects of telluric jitter

2.6 PRVS Pathfinder

The achievement of m/s radial velocity precisions using common-user telescopes is one of the major technological breakthroughs of recent years. This achievement must not be taken lightly. It was only possible following hardware and software systems coordinated over many years. Precision radial velocity techniques have been developed and improved using locally available equipment where new techniques and equipment maybe tested and integrated. The path from solar observation[5,6] to pioneering stellar observations using HF gas cells[7] to today's achievement of sub m/s RMS velocities, e.g., Keck+HIRES, ESO3.6m+HARPS, HET+HRS, AAT-UCLES and VLT-UVES is one that leads through several spectrographs, detectors and revisions of calibration and observing methodology. Moving into a wavelength regime where there is no tradition of radial velocities means there is relatively little legacy work and that the PRVS project is exceedingly challenging. It is unrealistic that we can foresee and fully specify all the real world pitfalls and interactions that need to be overcome in over to achieve 1 m/s radial velocities in the infrared. Thus significant resources were put toward a pathfinder project to validate design decisions. In the first phase this is a laboratory based experiment to measure earth rotation by intensive measurements of the Sun. During the PRVS design study we[8] built a simple version of PRVS which has already gained RMS precisions of better than 5 m/s in 1 minute on the Sun in the Y band (see Figure 6.) giving us confidence that the stated opto-mechanical errors of PRVS maybe achieved.

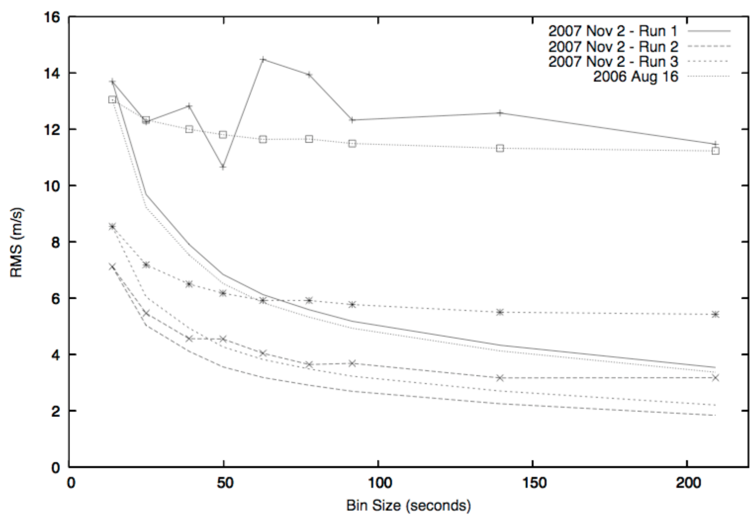

Figure 6. RMS values in m/s for the three observational sequences of 2006 and 2007 data sets (with data points) with various amounts of binning, along with the theoretical N (no data points) drop in the measured RMS for acch run. While the exposures are all 10-s each read-out time increases the time between successive images to 14s.

3. EXPECTATIONS FOR PRVS

An infrared RV survey will survey stars which span a mass range of at least a factor of 5, from ~0.08–0.4 $M_\odot$. This is comparable to the mass range currently being surveyed by current optical RV programs (~0.4–1.5 $M_\odot$) and illustrates the significant parameter space to be explored by PRVS. Three major scientific areas can be addressed by a PRVS survey: (1) predictions for giant and terrestrial planet formation, (2) incidence of terrestrial planets in their habitable zones and (3) the discovery of exoplanets within the reach of direct imaging.

There are a number of theoretical simulations which simulate the incidence of terrestrial exoplanets including analytical extrapolation[9], scaling laws[10], ab inito Monte Carlo methodology[11] as well the potential for exoplanets around M dwarfs as a means to distinguish formation mechanisms[12,13]. Theoretical works are generally optimistic about the formation of large numbers of terrestrial planets. While these are exciting and suggestive, the predictions include a wide variety of orbital outcomes and there remain many poorly constrained inputs to the models. Thus their predictive power is rather uncertain and given that the field of exoplanets has been driven to date by observations we consider a more empirical approach.

If we consider exoplanets discovered with orbits less than five years the Keck, Lick and AAT planet searches have surveyed 1040 stars and found 124 exoplanets. Potential PRVS discoveries can then be rescaled in mass to move from detection around Solar type stars (median value 1.1 $M_{\odot}$) to detection around 0.15 $M_{\odot}$(~M5V) and from 3 to perhaps 1 m/s and then be dependent on the mass function for a lower mass set of radial velocity targets. Given this is a completely unexplored regime the practicalities of local available objects (Figure 7) and spectral information (Figure 8) are crucial to a viable survey.

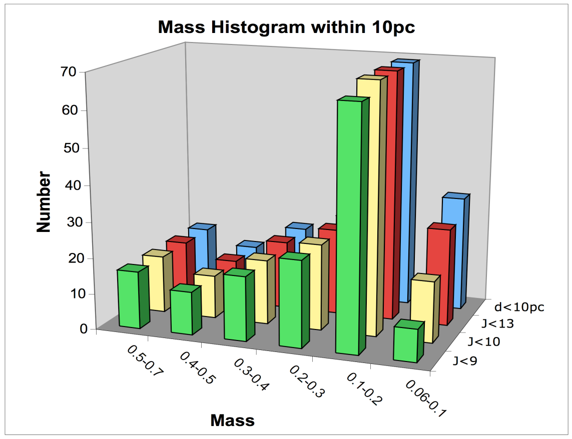

Figure 7. Examination of the 10pc sample indicates that the bulk of the available objects have masses less than 0.2 $M_{\odot}$ and are thus prime targets. The histograms are shown for different J band magnitudes to indicate that high precisions (e.g., S/N=150 in 1hr for J=11.3) will be achievable for all but the very coolest known brown dwarfs. Even this 10pc sample is expected to be incomplete by perhaps 50% and it is expected that the 0.06-0.1 $M_{\odot}$ bin will provide more objects than the 0.1-0.2 $M_{\odot}$ bin. This will be revealed following the analysis of deeper more precise surveys including proper motions (e.g., UKIDSS and Pann-Starrs).

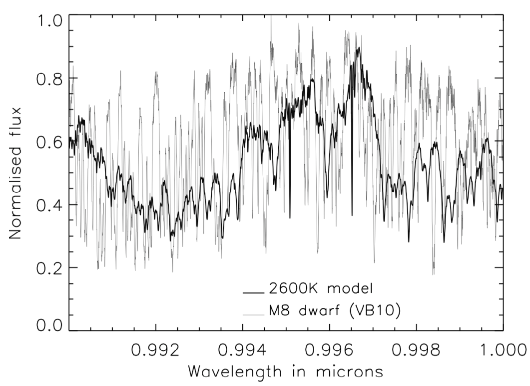

Figure 8. HIRES data[14] (thin line, S/N>100) for VB10 the archetypal late-type M dwarf indicates the large amount of radial velocity information available in late-type M dwarfs and is compared to synthetic spectra[15] (thick line). The poor match between data and observation arises from the lack of high quality molecular line lists appropriate for modelling cool star.

3.1 Mock Survey

In order to gauge the practicality of conducting a high-precision RV survey in the infrared we construct a notional survey. The input population of ultra-cool dwarfs in the solar neighbourhood was based on the *Nstars* project[16] and the observed IR colours and magnitudes of M and L dwarfs. Our analysis is based on the Bouchy et al. (2001)[17] formulation which indicates that for our theoretical models a S/N of 300 is required to each a velocity precision of ~ 1 m/s. As an independent check we have used RV code to extract radial velocities from synthetic spectra and produce very similar results. The limited real data that we have acquired from HIRES, PHOENIX, NIRSPEC and CGS4 suggests that S/N of around 125 or less will suffice to reach 1 m/s (noting considerable sensitivity to spectral type and metallicity). As part of this testing process we also investigated the effect of telluric emission and absorption. Even for extreme cases where telluric features are given motions of 100m/s radial velocity information maybe recovered. Our simulations are based on 2mm of water and ignoring 30 km/s around telluric features deeper than 2% (we have not attempted correction[18]). They leave 87% (Y), 34% (J) and 58% (H) of the available PRVS wavelength region. Based on measurements of activity in M stars 30% in each luminosity bin are rejected[19]. We also reject M stars with v sin i > 10 km/s although our modelling shows that is not necessarily a significant hindrance to measuring precise radial velocities. There is no evidence for higher radial velocity jitter toward later spectral classes[20,21]. Indeed we expect the RV-scatter caused by stellar activity to be less when moving from optical to the IR. Paulson et al. (2002)[22] found the RV scatter in their Hyades RV data to be caused mainly by spots. Plage regions are less important. This result is confirmed by RV-monitoring of the very active star EK Dra[23]. Modelling suggests the difference in temperature between spots and photosphere to be ~200K for late-type M dwarfs[19] (as opposed to ~1500K for Solar type stars), so particularly in the infrared the contrast between photosphere and spot will be small. Guenther et al. (2006)[24] consider this will result in a factor of ~10 reduction in RV jitter. For low activity stars in the optical a major source of jitter is asteroseismology, for M dwarfs the p-p mode error is expected to reduce by a factor of 4 relative to the Sun (based on extrapolation[25]).

As expected for a survey spanning a factor of ~100 in absolute infrared magnitude, it is easy to observe many of early-/mid-M types at little cost in telescope time. The required amount of observing time for these bright targets is driven by the fixed overhead, not by the integration time, and hence there is a strong premium on minimising the observing overheads (e.g. target acquisition). Observing the coolest objects is very costly in observing time, not only because these objects are getting fainter but also because the measured LF is turning down.

Table 2. assumes fraction of sky observable = 0.66, fgood an ad hoc parameter which represents the fraction of stars useable for an RV survey (inactive and v sin i < 10 km/s) and ranges between 0.7 at M2 and falls to 0.1 by L0V, min-max integration per object = 60-4800.0 sec, limiting mags {Y,J,H} = 12.30, 11.75, 11.20, observing efficiency = 80.0%, fixed overhead/star/epoch = 180.0 sec, # of epochs = 30, max # of targets per LF bin = 90.0, max # of bright targets per LF bin = 90.0, hours of observing per night = 8.0, survey duration = 5.0 yrs, N* = # of stars observed in sample, <dist = max distance (pc) of targets for each LF bin. The table is based on Gemini but in principle the instrument could fibre feed a variety of Mauna Kea telescopes.

S/N :	**300**		**125**	
***v* sin *i* / km/s:**	**All**	**<10**	**All**	**<10**
~Sp. Type	**Number of stars**			
M2.5 V	77	90	90	90
M3.0 V	77	90	90	90
M4.0 V	77	90	90	90
M5.0 V	77	90	90	90
M6.0 V	77	58	90	90
M6.5 V	35	17	68	90
M8.0 V	10	5	80	59
M9.0 V	3	1	38	17
L1.0	1	0	15	1
Total	434	441	663	617

It would also be particularly interesting to probe even lower mass objects. For example, 20 m/s precision at $0.04M_{Sun}$ gives sensitivity to close orbiting exoplanets with a few Earth masses. Following the survey design above but using S/N=50 and making no constraint on v sin i or activity then for 124 nights per year one can survey 278 L and T dwarfs. While large allocations of telescope time are necessary the near-infrared fibre-fed nature of PRVS means that the observing load can be shared by more than one telescope.

3.2 Potential Legacy

It is hard to underrate the stunning scientific impact of high precision optical radial velocity studies. The aim is to extend this success into the infrared regime. Our modelling of M dwarf radial velocity signals and experimentation with our pathfinder instrument show that PRVS is feasible now and would be sensitive to Earth-mass planets in the habitable zones of the nearest stars. PRVS can help to constrain several exceedingly promising fields of exoplanetary science that might otherwise only be achieved at optical wavelengths by building another generation of larger telescopes. How do the properties of exoplanets change from Sun-like to low-mass stars? (Does the mass of the planets of low-mass stars simply scale with the mass of the central object? Do we find the same eccentricity distribution as in solar-mass stars? Do we find the same dependence with metallicity as in solar-mass stars?) Together with the optical surveys PRVS will enable the mass and metallicity dependence of planet formation to be thoroughly investigated.

REFERENCES

[1] Marcy, G., Butler, R.P., Fischer, D., Vogt, S., Wright, J.T., Tinney, C.G., Jones, H.R.A., Progress of Theoretical Physics Supplement 158, 24-42 (2005)
[2] Rivera, E.J., Lissauer, J.J., Butler, R.P., Marcy, G.W., Vogt, S., ApJ, 634, 625-640 (2005)
[3] Beaulieu, J.-P., and 72 colleagues, Nature 439, 437-440 (2006)
[4] Liu, M.C., Najita, J., Tokunaga, A.T., ApJ, 585, 372-391 (2003)
[5] Beckers, J.M., Nature, 260, 227-229 (1976)
[6] Koch, A., Woehl, H., A&A, 134, 134-138 (1984)
[7] Campbell, B., Walker, G.A.H., PASP, 91, 540-545 (1979)
[8] Ramsey, L.W., Barnes J., Redman, S., Jones, H., Wolszczan, A., Jenkins, J., PASP, in press (2008)
[9] Grether, D., Lineweaver, C.H., ApJ, 640, 1051-1062 (2006)
[10] Ida, S., Lin, D.N.C., arXiv:0802.1114 (2008)
[11] Mordasini, C., Alibert, Y., Benz, W., Naef, D., , arXiv:0710.5667 (2007)
[12] Laughlin, G., Bodenheimer, P., Adams, F.C., ApJ, 612, L73-L76 (2004)
[13] Kornet, K., Wolf, S., Rozyczka, M., A&A,458, 661-668 (2006)
[14] Reiners, A., Basri, G., ApJ, 644, 497-509 (2006)
[15] Brott, I., Hauschildt, P.H. ,The Three-Dimensional Universe with Gaia, 576, 565 (2005)
[16] Allen, P.R., Koerner, D.W., Reid, I.N., Trilling, D.E., AJ, 625, 385-397 (2005)
[17] Bouchy, F., Pepe, F., Queloz, D., A&A, 374, 733-739 (2001)
[18] Bailey, J., Simpson, A., Crisp, D., PASP, 119, 228-236 (2007)
[19] Rockenfeller, B., Bailer-Jones, C.A.L., Mundt, R., A&A, 448, 1111-1124 (2006)
[20] Wright, J.T., PASP, 117, 657-664 (2005)
[21] Endl, M., Cochran, W.D., Kurster, M., Paulson, D.B., Wittenmyer, R.A., MacQueen, P.J., Tull, R.G., ApJ, 649, 436-443 (2006)
[22] Paulson, D.B., Saar, S.H., Cochran, W.D., Hatzes, A.P., ApJ, 124, 572-582. (2002)
[23] Konig, B., Guenther, E.W., Woitas, J., Hatzes, A.P., A&A, 435, 215-223 (2005)
[24] Guenther, E. High Resolution Infrared Spectroscopy in Astronomy 487-492 (2005)
[25] O'Toole, S.J., Tinney, C.G., Jones, H.R.A., MNRAS, 386, 516-520 (2008)